Interaction of Bubbles with Solidification Interfaces

J. M. Papazian*
Grumman Aerospace Corporation, Bethpage, N.Y.
and
W. R. Wilcox†
Clarkson College of Technology, Potsdam, N.Y.

The behavior of bubbles at a dendritic solidification interface was studied during the coasting phase of a sounding rocket flight. Sequential photographs of the gradient freeze equipment showed nucleation, growth, and coalescence of bubbles at the moving interface during both the low-gravity and 1-*g* tests. In the 1-*g* tests, the bubbles were observed to detach from the interface and float to the top of the melt. However, in the low-gravity tests no bubble detachment from the interface or steady-state bubble motion occurred, and large voids were grown into the crystal. These observations are discussed in terms of the current theory of thermal migration of bubbles and in terms of their implications on the space processing of metals.

Introduction

THE control of gas bubbles is often an important concern of the metallurgist. Too much porosity or critically located voids can ruin a casting or weld; conversely, some common purification processes rely on gravity-driven gas bubble motion for their effectiveness. Various procedures for the control of gas evolution or subsequent processing operations have been developed to minimize the problem or to exploit the properties of bubbles in terrestrial operations. However, in a low-gravity environment, bubbles will behave in a significantly different manner, and they are expected to be more of a problem. A low-gravity environment is characterized by reduced buoyancy forces, a decreased hydrostatic head, decreased free convection, and increased dispersion of foreign particles. These factors generally lead to easier nucleation and slower motion of bubbles. In fact, more gas bubbles were found incorporated in space-processed materials in four of the Skylab experiments.[1-4] In contrast to our extensive terrestrial experience in control and manipulation of bubbles, we are not yet able to describe some of the rudimentary aspects of bubble behavior in microgravity. This knowledge will be needed before extensive space-processing operations can be undertaken.

The primary objectives of this experiment are to study the interaction of bubbles with a dendritic solidification interface and to make preliminary observations of the rate of migration of bubbles in a temperature gradient. These objectives are related to two of the obvious possibilities for production of void free materials in a gravity-free environment, namely, to rely on pushing of bubbles by the solidification interface itself or to pull the bubbles away from the interface by means of a thermal gradient. A third possible technique involving the imposition of artificial gravity fields has been studied previously[5-7] and would be amenable to analysis by standard techniques.

Various studies of the development of porosity during terrestrial solidification process have been made; this topic is treated in standard texts.[8,9] In addition, observations of particle or bubble-interface interactions have been carried out using transparent systems by several researchers[10-14]; these studies will not be reviewed here. All of these studies were performed under 1-*g* conditions.

Experimental Procedure

This experiment was performed by directionally solidifying carbon tetrabromide using a gradient freeze technique. The carbon tetrabromide was previously saturated with various gases, these gases were then rejected during solidification and formed bubbles at the growth interface. Observation of the growth and motion of these bubbles was the primary objective of this experiment.

Carbon tetrabromide is a member of the class of materials known as "plastic crystals," characterized by a relatively low entropy of melting and a subsequent lower temperature phase transformation to a second, less plastic, crystal phase. The most important characteristic for our purposes is the low entropy of melting, which results in a dendritic rather than a faceted solidification interface and therefore "models" the solidification of typical metals. The main advantage of using CBr_4 lies in the transparency of the liquid phase and the relatively low melting point (90°C). These characteristics allowed us to construct a relatively simple apparatus in which the progress of solidification could be followed photographically during the "low-gravity" interval.

It should be borne in mind that the Black Brandt sounding rocket mission profile provides approximately 300 s during which all imposed accelerations are less than 10^{-4} *g*. This "low-gravity" interval is preceded by approximately 60 s of violent accelerations due to engine thrust, spin stabilization, despin, and a complex vibration spectrum and then followed by tumbling re-entry and the shock of an uncushioned landing. A rapidly changing vacuum and thermal profile also is imposed upon the apparatus by the rocket trajectory. These considerations limit experimenters to relatively simple and rapid experiments performed automatically by robust equipment. In addition, one must take into account the motions that are induced in liquid phases as a result of the accelerations before and after "low gravity." This motion was a cause of concern in this experiment because the specimens were launched in a half-liquid half-solid state. This configuration was chosen in the interest of experimental simplicity, as it allowed the apparatus design to provide for heating, temperature control, and equilibration prior to launch using ground-supplied power. Upon launch, the electrical connections were severed, and the apparatus was allowed to cool; the cooling rate was adjusted prior to flight by manipulation of the thermal loss paths. This resulted in an apparatus of minimum complexity and low power

Presented as Paper 77-194 at the AIAA 15th Aerospace Sciences Meeting, Los Angeles, Calif., Jan. 24-26, 1977; submitted Feb. 7, 1977; revision received Aug. 24, 1977.

Index categories: Space Processing; Materials, Properties of.

*Senior Research Scientist, Materials and Structural Mechanics, Research Department.

†Professor and Chairman, Chemical Engineering Department. Member AIAA.

requirements but involved the penalty of launching the specimens in a half-liquid half-solid state. The consequences of this will be discussed in the "Results" section.

The apparatus constructed for this experiment is shown in Fig. 1. It consists of four major parts. (A) is a GFE motorized 250-exposire 35-mm Nikon F2 camera contained in a supporting box. The camera used a Nikon 55-mm Micro lens set to photograph at ½ × magnification. (B) is the supporting structure, which houses the three other components and attaches directly to the mounting tabs of the rocket. It is approximately 14 in. diam × 16 in. high. (C) is the sample holder/heater assembly. This consists of an aluminum block, which accommodated the four 10- × 100-mm sample tubes, housed the lighting system, and contained the heaters. The heaters were located at the top and bottom of the block and were powered by 110 V ac through the umbilical cable. The temperatures of the top and bottom portions of the specimen holder were preset and controlled independently by two temperature controllers housed in the ground-support equipment electronic package. Specimen temperature measurements were made by an array of 14 thermistors, which were bonded to the back of the specimen holder. (D) is the electronics package, which contains an analog timer-sequencer controlling the operation of the camera and lights, a power supply for the camera and lights, and a 15-channel signal conditioner to convert the thermistor outputs to a 0-5 V dc signal suitable for the rocket's telemetry system. The electronics package was powered by the main onboard 28 V rocket battery and started by the liftoff switch. In operation, the heaters were activated 30 to 45 min before launch, and thereby a stable temperature gradient of 5°C/cm was established and maintained along the length of the specimen holder. The liquid-solid interface came to equilibrium at the 90°C locus, which was approximately one-half way up the specimen holder. Upon launch, the umbilical connection was ruptured, and the specimen holder began to cool at a rate determined by the ambient temperature and pressure and by the thermal conductivity of the specimen holder mounts. This was adjusted in the laboratory to provide approximately the desired solidification rate of 10 μm/s. The camera and lights came on automatically at 100 s after liftoff; 220 exposures were taken at a rate of approximately 1 frame/s.

The carbon tetrabromide was of commercial purity from lot A4C of Eastman Chemicals. The samples were contained in 10- × 100-mm pyrex tubes, which were sealed at one end by a glassblower. The seal at the other end was effected by a nylon stopper having two "O" rings. The stopper was at the bottom (cold) end of the tube. Numerous ground-based simulation (GBS) tests were performed to establish conditions of sample preparation which would insure reliable and

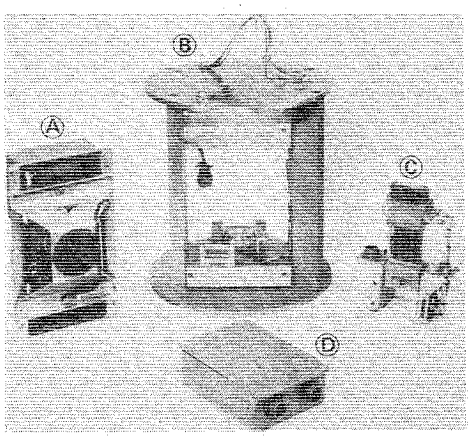

Fig. 1 The sounding rocket apparatus constructed for this experiment. The four major constituents are (A) the camera; (B) the supporting structure, 14 in. diam × 16 in. high; (C) the sample holder/heater assembly; and (D) the electronics package.

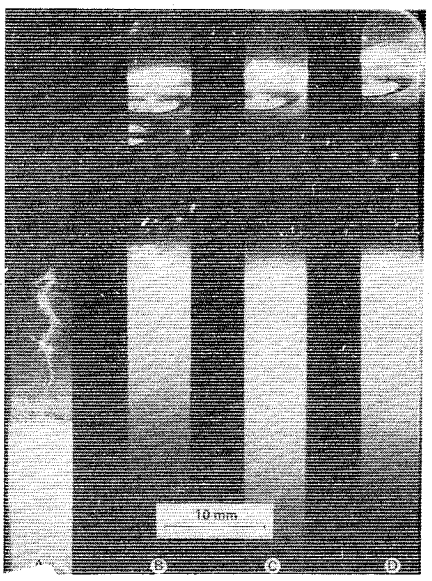

Fig. 2 Appearance of the specimens at $t = 88$ s after liftoff. The lower portions of the specimens (bright areas) are solid, and the upper portions (dark areas) are liquid.

copious evolution of bubbles at the solidification interface during the experiment. The preparation sequence finally chosen was as follows: 1) melting of as-received crystalline CBr_4 in the sample tube in a thermostatically controlled 95°C furnace; 2) bubbling of Ar, H_2, or N_2 through the molten CBr_4 for 5 min; and 3) stopper insertion and rapid cooling. All of these manipulations were carried out in an argon-filled dry box, which was shielded from short-wavelength light by filters. It previously had been determined that liquid CBr_4 decomposes rapidly in the presence of light. Numerous reactions are possible; in most cases, highly reactive radicals and bromine are produced. These reaction products caused rapid discoloration of the specimen and vigorously attacked the stopper and "O" rings. In order to suppress this photolysis, filters were installed on the specimen holder and dry box such that no light with a wavelength of less than 420-nm could reach the specimen. In addition, dwell time in the liquid state was kept to a minimum. The gas-filled volume in the sample tube (ullage) was adjusted to be approximately zero when the sample was half-liquid half-solid, the anticipated launch configuration.

Results

A. Initial Observations

During the actual rocket flight, the apparatus functioned properly, and the experiment was performed according to plan. The major results of this experiment are contained in the 220-exposure 35-mm film, which was taken during flight. The camera began framing at 80 s after liftoff and recorded at the rate of approximately 1 frame/s. This time-lapse sequence of pictures has been made into a 16-mm film.‡ Each original image was repeated eight times on the 16-mm film in order partially to adjust the 1-frame/s filming rate to normal projection rate (24 frames/s). Thus, when viewing the film, the acutal experiment is speeded up by a factor of 3. Initial observations of the film show significant generation, motion, and inclusion of bubbles in the mushy zone, the slow disappearance of small bubbles in the liquid, and no detectable motion of bubbles in the quiescent liquid. In addition to the film record, other data were generated by analysis of the returned specimens. Results from these two sources of information are discussed below.

‡One copy of this film has been submitted to the SPAR program office at Marshall Space Flight Center. A loan copy is available to interested parties from the authors.

B. Photographic Observations

One frame from the 220-exposure sequence is reproduced in Fig. 2, which shows the appearance of the samples at $t = 88$ s. The extreme left-hand tube, specimen A, is from experiment 74-15 of MIT, which contained naphthalene with various small particles added. The next tube, specimen B, was argon-saturated CBr_4; specimen C was hydrogen-saturated CBr_4, and specimen D was nitrogen-saturated CBr_4. All of the specimens were situated in the same thermal gradient of approximately 5°C/cm. The bottoms of the specimens were at the cool end, and thus the lower portions of all of the specimens were solid. (Naphthalene melts at 80°C, and carbon tetrabromide melts at 90°C.) The full 10-mm diam and 100-mm length of each sample tube is not visible in this photograph; it is obscured partly by the aluminum block assembly. The actual area visible is approximately 6.5×45-mm/sample tube.

Specimen A shows a vortexlike structure in the liquid just ahead of the interface. This feature is interpreted as being the image of small particles that were resting on the liquid-solid interface before launch and that were swept up by fluid motion during rocket spin and despin. The shape of this feature does not change during the 220-s series of photographs. This observation leads to the conclusions that 1) significant fluid motion occurred during launch, 2) the fluid motion was predominately axial rather than longitudinal, and 3) fluid motion has been damped out by $t = 80$ s. The viscosity of naphthalene varies from 0.97 at 80°C to 0.78 at 100°C, and microgravity was not established completely until approximately $t = 75$ s. Thus the damping occurred very rapidly, even more rapidly than had been expected. Comparison with photographs taken immediately before launch shows that the fluid motion during launch caused approximately 1 to 2 mm of melting back or erosion of the solid-liquid interface in the CBr_4 specimens.

Specimens B, C, and D contained bubbles in the liquid portion of the sample tubes. The images of the bubbles all were distorted by the cylindrical sample tubes. Control experiments in which transparent plastic spheres were photographed at different positions in the sample tube showed that a spherical object is distorted such that the vertical dimension (along the length of the tube) is unchanged but the horizontal dimension is magnified. Thus, the bubbles were in fact spherical and had a diameter equal to their apparent height.

Large bubbles of approximately 4-mm diam were present in all three tubes, and smaller bubbles, down to 40 μm diam, were present in tubes B and D. The bubbles were generated during the launch phase of the flight and probably were dispersed through the liquid by buoyancy and launch-induced fluid motion. The bubbles could have been due to evolution of trapped gas during melt-back, nucleation and growth of bubbles of gaseous solute rejected during solidification, or dispersal of gas present before launch. It seems likely that the 4-mm bubbles near the top of each tube were gas that had been pushed down from the top of the tube by launch-induced fliud motion and that the smaller bubbles were generated by the other two mechanisms.

Inspection of subsequent photographs in the flight sequence shows that during the course of the experiment many of the smaller bubbles slowly disappeared. The bubbles at the interface grew larger and were incorporated into the growing crystal as the experiment proceeded. These observations are much more apparent in the motion picture. Figure 3 is a photograph of a montage that was made by cutting out the picture of specimen D from 8- $\times$10-in. prints of selected frames and pasting these cutouts together. The composite shows the sequence of events more clearly than individual still photographs. This figure shows that there was no detectable motion of those bubbles that did not contract the interface. This was confirmed by use of a film motion analyzer. Figure 3 also shows that nucleation and growth of bubbles occurred at the advancing interface and that these bubbles sometimes

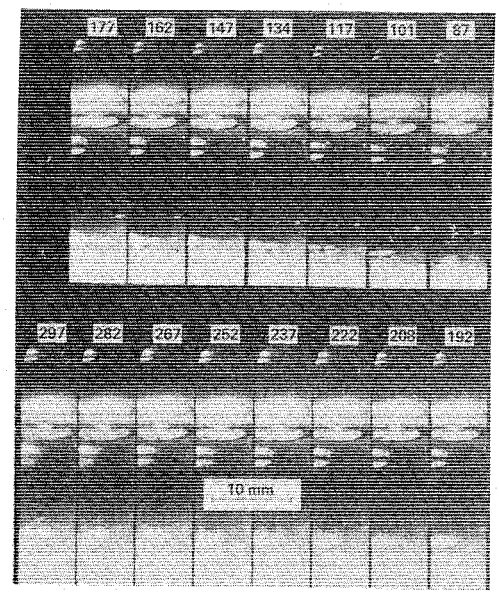

Fig. 3 Composite photograph of specimen B showing the progress of solidification in low gravity. The time since liftoff is shown for each view.

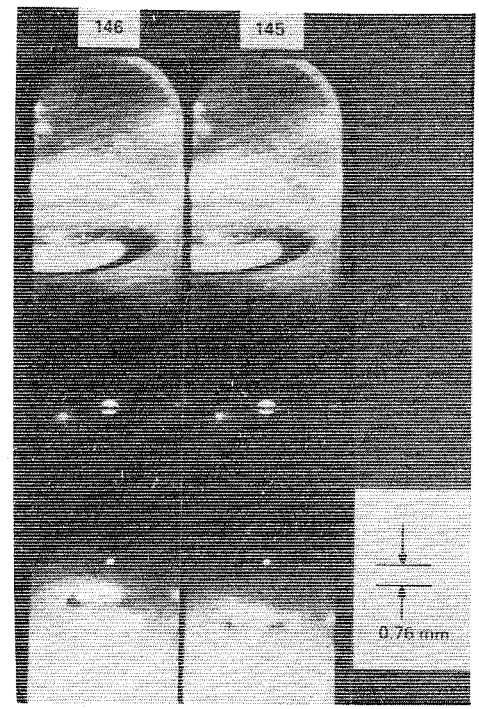

Fig. 4 A sequence of two views of specimen D taken 1 s apart. Note the abrupt motion of the large bubble at the solid-liquid interface.

were displaced. This behavior was observed in all three of the flight specimens.

The motion of bubbles at the interface was sometimes abrupt, as is obvious in the motion picture. A particular example is shown in Fig. 4, which shows two sequential views of specimen D. The two views were taken 1 s apart, and the bubble moved 0.8-mm in that time. It was stationary for many frames before and after. The ground-based simulation specimens produced almost no incorporation of bubbles at the interface. Numerous bubbles were generated at the interface, but they eventually were detached and rose rapidly under the influence of normal buoyancy forces.

Several small bubbles disappeared in the first 30 to 50 s, particularly in specimens B and D. These bubbles were situated in a portion of the melt well ahead of the solidification interface and gradually decreased in size and

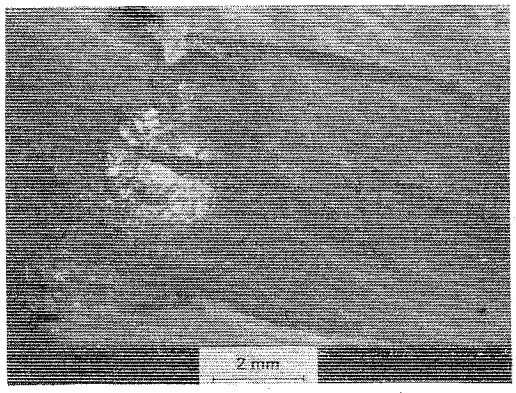

Fig. 5 Transmission macrograph of specimen D showing a large internal void (arrowed). The melt-back interface is roughly vertical and located on the left side of the picture; the growth direction is toward the right.

eventually disappeared. The liquid around the bubbles was cooling slowly. There are two possible explanations for the dissolution of these gas bubbles:

1) The gas solubility increases with decreasing temperature.
2) The melt was not saturated with gas.

With no knowledge of gas solubilities in CBr_4 and no knowledge of convective mixing during the melt-back phase of the ground, we cannot tell which mechanism predominated.

The flight film allows us to measure the growth rate of the specimens. It is sometimes difficult to decide exactly where the crystals end and the liquid begins. This not unusual, since the material was not particularly pure, and an extensive dendritic mushy zone was expected and found. Also, the lighting system was designed for bubble observations and was not optimum for observing the interface. However, we can define subjectively three "interfaces," namely, the fastest dendrite tip, a transparent interface, and a translucent interface. Measurements of the positions of these interfaces were made for each specimen. The average growth rates of these three "interfaces" are 110, 10, and 4 μm/s, respectively. Measurements on the two other flight specimens gave similar values. Similar data for a ground-based simulation specimen gave values of 2.5 and 120 μm/s for the transparent and fastest dendrite interfaces.

C. Structural Observations

All three of the flight specimens contained voids in the portion of the crystal which was grown during the microgravity interval. These were documented by means of x-ray shadowgraphs. The GBS specimens did not contain macroscopic voids. Figure 5 is a macrograph of flight specimen D in which part of a subsurface void is visible. This picture was taken using transmitted light, with the specimen still encapsulated in its pyrex tube. The circumference of the crystal was complete in all cases; i.e., the voids were confined to the center of the crystal and did not intersect the external surface.

During microscopic investigations, the misorientation across grain boundaries can be seen readily from the dendritic pattern in each crystal. The pattern probably was caused by segregation of impurities to the regions between dendrite arms. The grains were generally of a columnar morphology. Using these observations as a guide, the grain size of the specimens was estimated by simply counting the number of grain boundaries around the circumference of the specimen at the melt-back interface. The results are shown in Table 1. Note that the flight specimens were slightly finer grained than the GBS specimens.

Table 1 Grain size (mm) of three different type of specimens

	Ar	H_2	N_2
Flight	2.3	2.1	1.9
GBS Aug. 18, 1975	2.8	2.5	2.8
GBS Aug. 21, 1975	2.5	3.6	3.1
GBS Sept. 4, 1975	4.2	3.6	3.1

Discussion

The results of this experiment show, for the first time, generation, coalescence, and incorporation of bubbles at a solidification interface in the absence of buoyancy forces. The observations are not yet quantitative, nor do they form part of a coherent scientific description of the process of bubble-interface interaction. These tasks will be pursued on later flights. The motion picture record of the experiment adds an extra dimension of insight into the dynamics of the process. In addition, we have gained understanding of the sounding rocket environment.

The juxtaposition of 70 s of rapid spin, violent acceleration and thrust, followed by 300 s in which all imposed accelerations are less than 10^{-4} g, does not appear to preclude meaningful experiments. Fluid motion seems to have been significant during the launch phase, as evidenced by the particle-decorated vortex in sample A and the distribution of bubbles in samples B and D. The sample tube was aligned with the axis of the rocket and approximately 100 mm off center. Each tube had an i.d. of 8 mm and was launched with the hot end up. From the shape of the vortex and location of the bubbles, particularly the large bubbles, we conclude that the circumferential fluid velocity (i.e., in the plane normal to the rocket axis) was significantly greater than the axial velocity (along the axis of the rocket). Thus, there was significant interface erosion or melt-back, but the fluid motion was not vigorous enough to level the temperature gradient completely or distribute the foreign bodies throughout the liquid. Some leveling of the temperature gradient must have occurred, but our temperature measurements were made on the aluminum block, not inside the specimen capsules, and are therefore of little use in determining how much leveling occurred. It is thought, however, that a substantial temperature gradient remained in the liquid at the beginning of the microgravity interval.

The damping of fluid motion was extremely rapid. Despin occurred at approximately 64 s, and the rate control system was activated immediately afterward; microgravity conditions were fully established by 75 s. Our first photograph at 80 s showed no evidence of fluid motion; this macroscopically quiescent state persisted to the end of the experiment at approximately 300 s.

The ease with which numerous large bubbles were incorporated into the portions of the specimens grown during the microgravity interval is not particularly surprising. Previous work has shown that only below a critical (low) growth rate are small bubbles rejected from solidification interfaces during faceted growth. Bubble pushing by dendritic interfaces should be relatively more difficult. Furthermore, the incorporation of porosity or large voids in terrestrial castings is not unusual. The absence of a buoyancy force makes the generation of voids during the solidification of gas-bearing liquid metals even more likely during space-processing operations, as evidenced by our results.

The most surprising observation of this experiment was the immobility of bubbles in a temperature gradient in the absence of gravity. The only previous work in this field[15] leads to the prediction that bubbles should move with a velocity v, given approximately by

$$v = \frac{d\gamma}{dT} \cdot \frac{dT}{dz} \cdot \frac{r}{3\mu} \tag{1}$$

or

$$Re = M/3 \tag{2}$$

where $d\gamma/dT$ is the temperature dependence of the surface tension, dT/dz the imposed temperature gradient, r the

bubble radius, μ the fluid viscosity, *Re* the Reynolds number, and *M* the Marangoni number. For a 1-mm bubble with $d\gamma/dT = -0.1$ dyn/cm-°C, $dT/dz = 5$°C/cm, and $\mu = 2$ cp, this formula gives an expected velocity of about 4 mm/s. This prediction is not borne out in our experiment. Motion analysis of the bubble positions given an upper limit for a possible velocity of approximately 10^{-2} mm/s. There are several reasons why the observed bubble immobility may be an experimental artifact; these are discussed in turn:

1) $d\gamma/dT = 0$. If the surface tension of CBr_4 does not vary with temperature in the region of interest, then there would be no driving force for bubble migration. However, we have measured $d\gamma/dT$ for our CBr_4 in the laboratory under conditions that should approximate those of the flight experiment. The results show a temperature dependence of $d\gamma/dT = -0.11$ dyn/cm-°C, a fairly typical value for organic liquids.

2) $dT/dz = 0$. If no temperature gradient were present, there would be no driving force for migration. A stable temperature gradient certainly existed before launch, but perhaps this was eliminated almost completely by launch-induced fluid motion. As discussed previously, fluid motion did take place, and some leveling of the temperature gradient was observed. The imposed accelerations were primarily downward, because of liftoff, and radial, because of spin and despin. The longitudinal forces would not tend to cause much mixing, since the denser (cooler) fluid was at the bottom. Transient spin can be very effective at mixing, but in this case it did not seem to have been, as evidenced by the position of the particles in specimen A. Thus, it is thought that the temperature gradient was not leveled completely. Furthermore, since all of the heat loss occurred through the ends of the specimen, the temperature gradient would have been reestablished during flight.

3) Pinning. If the bubbles were pinned by being in contact with the tube wall or solid material, then they would not have been free to migrate. It is possible that during despin the preexisting bubbles were thrown to the tube walls and thus unable to move. It is difficult to evaluate the likelihood of this situation.

4) Impurity segregation. It is possible that impurities could have segregated to the surface and arrested bubble motion. We distinguish between two cases: a) the lack of an energetic driving force due to equilibrium segregation, and b) a kinetic limitation on the rate of matter transport. Equilibrium segregation, as defined in Ref. 16, is limited to coverages on the order of a monolayer[17] and is strongly temperature-dependent. This strong temperature dependence of absorption can lead to a $d\gamma/dT = 0$ or even $d\gamma/dT > 0$.[18,19] This naturally would cause the bubble to be static or to migrate in the opposite direction. We do not believe this to have been the case in this experiment because our laboratory measurements of $d\gamma/dT$ would have shown this effect.

A kinetic limitation might have arisen if an impurity were present which formed a film at the bubble surface, and if the rate of transport of an impurity molecule between the segregated layer and the bulk liquid were slow. This film would inhibit the motion of molecules in the surface. This situation has been observed in bubble buoyancy experiments and might account for greatly reduced migration rates even though a negative $d\gamma/dT$ still existed. In summary, there are several possible explanations for the observed bubble immobility; it is hoped that the two subsequent flights of this experiment will provide more information on this question.

Summary

The effect of gravity on the grown-in void content in our CBr_4 specimens strikingly illustrates the potential problem posed by bubble generation during solidification in the orbital environment. We have observed that during terrestrial solidification bubbles nucleate and grow at the interface but generally detach and float to the surface of the melt. Thus, we usually obtain a specimen that is free of large voids. However, in freefall, bubble nucleation and growth also occur, but the bubbles do not detach from the interface, and the dendritic growth front is able to go around the bubbles, thus forming a void.

Coalescence of bubbles trapped in the mushy zone was observed to occur in an abrupt manner, similar to the collapse of soap films. The grain size of the low-gravity specimens was finer than that of the GBS specimens. Bubbles, 50 μm to 4 mm diam, situated in the melt well ahead of the interface did not migrate to the hot end of the sample tube; this is contrary to the predictions of thermal migration of bubbles in the absence of gravity. Several possible explanations for this behavior are given.

Acknowledgment

The authors wish to acknowledge the assistance of S. A. Chou, R. M. Gutowski, G. Knoflicek, and M. Kesselman. This research was partially supported by NASA Contract NAS8-31529.

References

[1] Yee, J. F., Sen, S., Samra, K., Lin, Mu-C., and Wilcox, W. R., "Directional Solidification of InSb-GaSb Alloys," *Proceedings of the Third Space Processing Symposium*, Huntsville, Ala., 1974, p. 301.

[2] Larson, D. J., "Skylab M553 Sphere Forming Experiment," *Proceedings of the Third Space Processing Symposium*, Huntsville, Ala., 1974, p. 101.

[3] Deruyttere, A., Aernoudt, E., Gueminne, M., Smeesters, J., Arkens, O., and Verhaeghen, M., "M565 Silver Grids Melted in Space," *Proceedings of the Third Space Processing Symposium*, Huntsville, Ala., 1974, p. 159.

[4] Kawada, T., Takahaski, S., Yoshida, S., Ozaqa, E., and Yoda, R., "Preparation of a Silicon Carbide Whisker Reinforced Silver Composite Material in a Weightless Environment," *Proceedings of the Third Space Processing Symposium*, Huntsville, Ala., 1974, p. 203.

[5] Bauer, H. F., "Theoretical Investigation of Gas Management in Zero Gravity Space Manufacturing," Final Rept. on Contract NAS 8-25179, NASA Marshall Space Flight Center, Huntsville, Ala., Oct. 1970.

[6] Bauer, H. F., "Motion of a Large Gas Bubble under the Lack of Gravity in a Rotating Liquid," *AIAA Journal*, Vol. 9, July 1971, p. 1426.

[7] Bauer, H. F. and Siekmann, J., "On the Shape of a Rotating Fluid System Consisting of a Gas Bubble Enclosed in a Liquid Globe," *Zeitschrift fur angewandte Mathematik und Physik*, Vol. 22, 1971, p. 532.

[8] Chalmers, B., *Principles of Solidification*, Wiley, New York, 1964.

[9] Flemmings, M. C., *Solidification Processing*, McGraw-Hill, New York, 1974.

[10] Uhlman, D. R., Chalmers, B., and Jackson, K. A., "Interaction Between Particles and a Solid-Liquid Interface," *Journal of Applied Physics*, Vol. 35, No. 10, Oct. 1964, p. 2986.

[11] Rocquet, P., Rossi, J. C., and Adam-Gironne, J., "Comparative Quality on Flat Rolled Products Produced from Continuously Cast and Conventionally Rolled Steels," *Journal of Metals*, Aug. 1967, pp. 57-61.

[12] Rocquet, P., Adam-Gironne, J., and Rossi, J. C., "Recherches sur L'Effervescence Lors de la Solidification De L'Acier," *Revue de Métallurgie*, Vol. 4, April 1968, p. 257.

[13] Cisse, J. and Bolling, G. F., "A Study of the Trapping and Rejection of Insoluble Particles during the Freezing of Water," *Journal of Crystal Growth*, Vol. 10, 1971, p. 67.

[14] Vasconcellos, K. F. and Beech, J., "The Development of Blowholes in the Ice/Water/Carbon Dioxide System," *Journal of Crystal Growth*, Vol. 28, 1975, p. 85.

[15] Young, N. O., Goldstein, J. S., and Block, M. J., "The Motion of Bubbles in a Vertical Temperature Gradient," *Journal of Fluid Mechanics*, Vol. 6, 1959, p. 350.

[16] McLean, D., *Grain Boundaries in Metals*, Oxford Univ. Press, London, 1957, p. 116.

[17] Cahn, J. W. and Hillard, J. E., "On the Equilibrium Segregation at a Grain Boundary," *Acta Metallurgica*, Vol. 7, 1959, p. 219.

[18] Jones, H. and Leak, G. M., "The Surface Entropy of Solid Metals," *Metal Science Journal*, Vol. 1, 1967, p. 211.

[19] Jones, H. and Leak, G. M., "The Effect of Surface Adsorbtion on Zero Creep Measurements in Iron-Silicon Alloys," *Acta Metallurgica*, Vol. 14, 1966, p. 21.